

***s*-channel discontinuities and the two-Reggeon cut\***Thomas A. DeGrand<sup>†</sup>*Laboratory for Nuclear Science and Department of Physics, Massachusetts Institute of Technology, Cambridge, Massachusetts 02139<sup>‡</sup>  
and Department of Theoretical Physics, University of Geneva, Geneva, Switzerland*

(Received 13 January 1975)

We make a detailed calculation of the *s*-channel discontinuities of the two-Reggeon cut in order to see how the singularities of the Reggeon-particle vertices affect the weight with which an intermediate state contributes to the cutlike part of the amplitude. We confirm the counting of Halliday and Sachrajda for the Mandelstam graph and show the extent to which this result can be applied to more general cut diagrams so that the results of Abramovskii, Gribov, and Kancheli hold. We also consider amplitudes with vertices constructed from the precepts of multi-Regge theory (for instance, from a dual model) in which the counting of terms is different: In particular, the simultaneous discontinuity through both Reggeons does not contribute to the cut. The weight of a given *n*-particle intermediate state in forming the cut depends crucially on the analytic properties of the vertex one chooses.

## I. INTRODUCTION

The problem of Regge cuts is an old one. Although cuts were first discussed as early as 1962 by Amati, Fubini, and Stanghellini,<sup>1</sup> it was Mandelstam<sup>2</sup> who in 1963 found a Feynman graph in weakly-coupled  $\phi^3$  theory which possessed cutlike behavior. In recent years, Regge cuts have been studied not only in field theory but also in the framework of analytic S-matrix theory. These investigations were pioneered by the work of Gribov, Pomeranchuk, and Ter-Martirosyan.<sup>3</sup> In this context, White<sup>4</sup> has proven that the Regge cut corresponding to the exchange of two Pomerons in the *t* channel contributes negatively to the total cross section, thereby reaffirming the field-theoretic result of Mandelstam.

These studies were carried out in the *t* channel. It is also possible to study Regge cuts in the *s* channel. There the problem is, on the one hand, simpler because one can use unitarity as an aid in one's investigation; however, this simplicity is negated by the fact that a Reggeon is a complicated object when viewed in the *s* channel. For instance, in field theory it is composed of sums of ladder graphs so that its intermediate state is made up of a very large number of particles.

The advantage of an *s*-channel approach to Regge cuts in two-to-two elastic scattering is that the imaginary part of the two-to-two amplitude is formed by taking the two-to-*n* particle amplitude, squaring it, and integrating over the *n*-particle intermediate phase space. This is just a consequence of unitarity. So one can take the Regge-cut amplitude, slice it in all possible ways so that all different intermediate states are put on the mass shell, and find what the contribution of the amplitude is to the total cross section by adding up the pieces. One finds that some slicings

are more important than others; these results can then be used to build models of production processes which, when squared, reproduce the dominant parts of the imaginary part of the two-to-two amplitude.

This program has been carried out by Abramovskii, Kancheli, and Gribov<sup>5</sup> in a general framework and in a detailed calculation of the Mandelstam graph by Halliday and Sachrajda.<sup>6</sup> They found that there are three types of slicings which are important in building up the cutlike asymptotic behavior of the Mandelstam graph. The first, shown in Fig. 2 and discussed in Sec. III, is a diffractive cut in which no Reggeons are sliced. The second type allows one Reggeon to be cut (see Fig. 8 and Sec. V), and the third slicing is one in which a discontinuity is taken across both Reggeons simultaneously (Fig. 5, Sec. IV). There are a total of two diffractive slicings, four one-Reggeon absorptive slicings, and one double slice. If the Reggeons are purely imaginary, as is assumed to be the case for Pomerons, slicing a Reggeon is equivalent to multiplying the amplitude by  $-2$ . If one assumes that the two-Reggeon-two-particle vertex is unaffected by the slicings (designating it as a constant *N*), then the discontinuities add up to give a cutlike asymptotic behavior to  $\text{Im}A$  which may be written schematically as

$$\begin{aligned}\text{Im}A &= 2N_1 N_2 + 4(-2)N_1 N_2 + 1(-2)(-2)N_1 N_2 \\ &= -2N_1 N_2,\end{aligned}$$

exactly the negative of the diffractive contribution.

However, we noticed that in order to compare the slices through one or both Reggeons with the diffractive slice, it was necessary to take a second discontinuity in the cluster mass in the two-Reggeon slice. The two discontinuities involve overlapping-channel invariants. Such double dis-

continuities often vanish for certain ranges of the kinematical variables. (It has been proven in perturbation theory that double discontinuities in overlapping kinematic variables vanish in the physical region of those variables.<sup>7</sup>) For the Mandelstam graph this is the case; however, the above counting is restored by the presence of anomalous singularities (triangle and end-point singularities) elsewhere in the complex plane. This restoration is so striking that one might wonder if it is unique to the Mandelstam graph. Indeed, one can write down Reggeon-particle couplings which possess only normal threshold singularities; then a counting of

$$\begin{aligned} \text{Im}A &= 2 \text{ (for diffractive slicings)} \\ &+ 2(-2) \text{ (one } -2 \text{ for slicing through} \\ &\quad \text{each Reggeon times} \\ &\quad \text{two Reggeons)} \\ &= -2 \end{aligned}$$

results, which again reverses the diffractive contribution. The different counting has the effect that a different set of production processes than those of the Mandelstam graph maybe regarded as important in generating the asymptotic cutlike behavior of the amplitude. These couplings, as well as those abstracted from field theory, may be used in the construction of a Reggeon calculus.

The outline of the paper is as follows: Section II introduces the kinematics and lays the groundwork for an analysis of the Mandelstam graph. Section III is a study of discontinuities in which no Reggeons are cut. In Secs. IV and V slicings of two and one Reggeon are considered. Section VI is a discussion of the generality of the Mandelstam graph results. Finally, in Sec. VII we investigate models (in particular, the dual model) of the Reggeon-particle vertex which give a different counting; the discussion is motivated by the assumption that such amplitudes lack second discontinuities in overlapping channels. If there is a single statement which this paper makes, it is that the singularity structure of the two-Reggeon-two-particle vertex, throughout the entire complex plane, is as important in determining the weight of some intermediate state of the two-Reggeon cut as is the singularity structure of the Reggeons.

II. KINEMATICS

The Mandelstam graph with its lines labeled for future use is shown in Fig. 1(a). It will be more convenient to redraw it in a planar form, Fig. 1(b); the outer box represents the lower part of

the graph in the first figure. The advantage of this picture is that the various slicings which will be taken can be seen more clearly; for instance, the presence of a slicing through lines  $q_5, q_6, q_7,$  and  $q_8$  is readily apparent.

The amplitude corresponding to the Mandelstam graph is

$$\begin{aligned} A(s, t) &= \frac{-i}{(2\pi)^8} \int \frac{\prod_{j=1}^4 d^4 q_j \delta^4(p_1 + p_2 - \sum_{j=1}^4 q_j)}{\prod_{i=1}^8 (q_i^2 - m_i^2 + i\epsilon)} \\ &\quad \times \xi_i \beta(t_i) s_i^{\alpha_i} \xi_r \beta(t_r) s_r^{\alpha_r}, \end{aligned} \quad (2.1)$$

with

$$\begin{aligned} s_i &= (q_2 + q_3)^2, \\ s_r &= (q_1 + q_4)^2, \\ t_l &= (q_5 - q_2)^2 = -q_{l\perp}^2, \\ t_r &= (q_1 - q_6)^2 = -q_{r\perp}^2, \\ s &= (p_1 + p_2)^2, \\ t &= (p_1 - p_3)^2, \end{aligned} \quad (2.2)$$

and  $\xi_i, \beta(t_i),$  and  $\alpha_i$  are the signature, vertex function, and trajectory functions of the  $i$ th Reggeon.

A more convenient parametrization, the Sudakov variables,<sup>8</sup> will be used in this work. We define

$$\begin{aligned} \vec{q}_i &= \alpha_i \vec{p}_\alpha + \beta_i \vec{p}_\beta + \vec{q}_{i\perp}, \\ p_\alpha &= (p_1 - p_2 m_1^2/s), \quad p_\beta = (p_2 - p_1 m_2^2/s), \\ q_{i\perp} \cdot p &= 0 \end{aligned} \quad (2.3)$$

$$q_i^2 - m_i^2 = \alpha_i \beta_i s - \mu_i^2, \quad \mu_i^2 = q_{i\perp}^2 + m_i^2, \quad (2.4)$$

$$d^4 q_i = \frac{1}{2} |s| d\alpha_i d\beta_i d^2 q_{i\perp}, \quad (2.5)$$

$$\begin{aligned} \delta^4(p_1 + p_2 - \sum q_i) &= \frac{2}{|s|} \delta(\sum \alpha_i - 1) \delta(\sum \beta_i - 1) \\ &\quad \times \delta^2(\sum q_{i\perp}). \end{aligned} \quad (2.6)$$

The amplitude (2.1) becomes

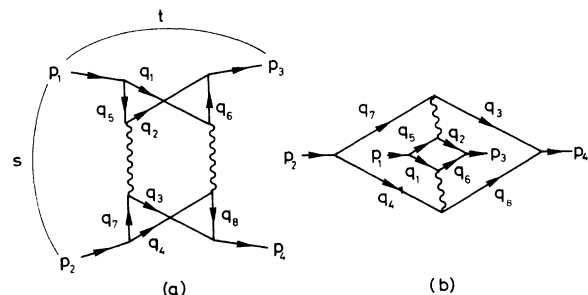


FIG. 1. The Mandelstam graph in (a) nonplanar and (b) planar form.

$$\begin{aligned}
A(s, t) = & \frac{-i}{(2\pi)^8} \frac{s^3}{8} \int \frac{\prod_{i=1}^4 d\alpha_i d\beta_i d^2 q_{i\perp} \delta(\sum \alpha_i - 1)}{\prod_{i=1}^8 (\alpha_i \beta_i s - \mu_i^2 + i\epsilon)} \\
& \times \delta(\sum \beta_i - 1) \delta^2(\sum q_{i\perp}) \\
& \times \beta(t_1) \xi_1 s_1^{\alpha_1} \beta(t_r) \xi_r s_r^{\alpha_r}.
\end{aligned} \tag{2.7}$$

The usefulness of Sudakov variables will shortly become apparent. The inverse propagator of line  $q_1$  is

$$q_1^2 - m_1^2 = \alpha_1 \beta_1 s - \mu_1^2, \tag{2.8}$$

and that of line  $q_5$  ( $= p_1 - q_1$ ) is

$$q_5^2 - m_5^2 = -(1 - \alpha_1)(\beta_1 s - d^2) - \mu_5^2, \tag{2.9}$$

where the Sudakov variables for the line  $p_1$  are  $\alpha = 1$ ,  $\beta = d^2/s$  (the mass of  $p_1$  is  $d$ ). In order for these propagators to remain finite as  $s$  goes to infinity  $\beta_1 \sim 1/s$  and so  $\alpha_1 \sim 1$ . Similarly, if the particle in the bottom lines of Fig. 1(a) is to have finite momenta,  $\beta_3$  and  $\beta_4$  must be of order unity and  $\alpha_3$  and  $\alpha_4$  of order  $1/s$ . These constraints are justified by the fact that the behavior of the amplitude at  $s \rightarrow \infty$  is sought, and the dominant part of the amplitude therefore occurs for  $q^2 \ll s$  on all internal legs.

The four-dimensional  $\delta$ -function factors:

$$\delta(\sum \alpha - 1) \delta(\sum \beta - 1) \rightarrow \delta(\alpha_1 + \alpha_2 - 1) \delta(\beta_3 + \beta_4 - 1). \tag{2.10}$$

$$\begin{aligned}
A(s, t) = & \frac{-is}{(2\pi)^8} \int \frac{dt_1 dt_r dM_1^2 dM_2^2 \theta(-\lambda)}{16[-\lambda(t, t_1, t_r)]^{1/2}} \frac{d\alpha_1 d\alpha_2 \delta(1 - \alpha_1 - \alpha_2) d\beta_2 d\alpha_4 d\beta_3 d\beta_4 \delta(1 - \beta_3 - \beta_4)}{\prod_{i=1}^8 (\alpha_i \beta_i s - \mu_i^2 + i\epsilon)} \\
& \times \beta(t_1) \xi_1 s_1^{\alpha_1} \beta(t_r) \xi_r s_r^{\alpha_r}.
\end{aligned} \tag{2.14}$$

As a final simplification one can do the integrations over the  $\delta$  functions to eliminate one  $\alpha$  and one  $\beta$ , change variables from  $\beta_2$  and  $\alpha_4$  to  $\beta_2 s$  and  $\alpha_4 s$ , and rewrite  $s_1$  and  $s_r$  in terms of  $s$ :

$$\begin{aligned}
s_r &= \alpha_1 \beta_4 s = \alpha_1 (1 - \beta_3) s, \\
s_1 &= \alpha_2 \beta_3 s = (1 - \alpha_1) \beta_3 s.
\end{aligned} \tag{2.15}$$

The amplitude becomes

$$\begin{aligned}
A(s, t) = & \frac{-i}{16(2\pi)^8} \int \frac{dt_1 dt_r \theta(-\lambda)}{\sqrt{-\lambda}} dM_1^2 dM_2^2 s^{\alpha_1 + \alpha_r - 1} \\
& \times B_1(M_1^2, t, t_1, t_r) B_2(M_2^2, t, t_1, t_r),
\end{aligned} \tag{2.16}$$

where

This factorization is just a statement that the two ends of the Reggeon are separated by a wide rapidity gap.

One could proceed at this point to a discussion of the discontinuities; however, it will be convenient to make a further change of variables to aid in a physical understanding of what is going on. Define the cluster masses of the two-Reggeon-two-particle vertices as

$$\begin{aligned}
M_1^2 &= (q_1 + q_2)^2 \\
&= (\beta_1 + \beta_2) s - (q_{1\perp} + q_{2\perp})^2 \\
&\equiv M_{1\perp}^2 - q_{1\perp}^2,
\end{aligned} \tag{2.11}$$

$$\begin{aligned}
M_2^2 &= (q_3 + q_4)^2 \\
&= (\alpha_3 + \alpha_4) s - (q_{3\perp} + q_{4\perp})^2 \\
&\equiv M_{2\perp}^2 - q_{1\perp}^2,
\end{aligned} \tag{2.12}$$

and change variables from  $\beta_1$  to  $M_{1\perp}^2/s - \beta_2$  and from  $\alpha_3$  to  $M_{2\perp}^2/s - \alpha_4$ . In addition, one of the four transverse integrations may be performed to eliminate the transverse  $\delta$  function and the other transformed to

$$d^2 q_{\perp} = \frac{dt_1 dt_r \theta(-\lambda)}{2[-\lambda(t, t_1, t_r)]^{1/2}}, \tag{2.13}$$

where

$$\lambda(x, y, z) = (x + y - z)^2 - 4xy.$$

The integral becomes

$$B_1 = \int \frac{d\alpha_1 d(\beta_2 s) d^2 q_{1\perp} (\alpha_1)^{\alpha_r} (1 - \alpha_1)^{\alpha_1}}{\prod_{i=1,2,5,6} (q_i^2 - m_i^2 + i\epsilon)}, \tag{2.17a}$$

$$B_2 = \int \frac{d\beta_3 d(\alpha_4 s) d^2 q_{4\perp} (\beta_3)^{\alpha_1} (1 - \beta_3)^{\alpha_r}}{\prod_{i=3,4,7,8} (q_i^2 - m_i^2 + i\epsilon)}. \tag{2.17b}$$

The first part of this expression is recognizable as the familiar phase-space integral for the double-Regge cut, the power behavior of  $s$  is cutlike, and the final expressions are the two-Reggeon-two-particle vertices, which are functions of  $M_1^2$  or  $M_2^2$  and  $t, t_1, t_r$ . This particular form of the amplitude is valid only for the limit  $M^2/s \rightarrow 0$  as  $s \rightarrow \infty$ , for only then does the longitudinal part of

the phase space, the  $\alpha$  and  $\beta$   $\delta$  functions, decouple. (A limit  $s \rightarrow \infty$  is implicitly assumed in writing the Jacobian as  $1/|s|$  in the transformation to Sudakov variables.) All the results derived here are valid only in that limit. One can imagine that the limits on the  $M^2$  integrals are not  $\pm\infty$  but some large mass  $M_0^2$ , where  $M^2 \ll M_0^2$  for  $M^2$  any characteristic mass associated with the particle propagators, but still with

$$M_0^2 \ll s. \quad (2.18)$$

(The integral over  $M^2$  must of course be convergent for large  $M^2$ .)

Finally, a list is provided of propagators and other kinematical variables for future reference. They are

$$\begin{aligned} q_1^2 - m_1^2 &= \alpha_1(M_{1\perp}^2 - \beta_2 s) - \mu_1^2, \\ q_2^2 - m_2^2 &= (1 - \alpha_1)\beta_2 s - \mu_2^2, \\ q_5^2 - m_5^2 &= -(1 - \alpha_1)(M_{1\perp}^2 - \beta_2 s - d^2) - \mu_5^2, \\ q_6^2 - m_6^2 &= -\alpha_1(\beta_2 s - d^2) - \mu_6^2, \\ q_3^2 - m_3^2 &= \beta_3(M_{2\perp}^2 - \alpha_4 s - d^2) - \mu_3^2, \\ q_4^2 - m_4^2 &= (1 - \beta_3)\alpha_4 s - \mu_4^2, \\ q_7^2 - m_7^2 &= -\beta_3(\alpha_4 s - d^2) - \mu_7^2, \\ q_8^2 - m_8^2 &= -(1 - \beta_3)(M_{2\perp}^2 - \alpha_4 s) - \mu_8^2, \end{aligned} \quad (2.19)$$

where  $(\vec{q}_\perp = \vec{q}_l + \vec{q}_r$  and  $l = -q_\perp^2$ ),

$$\begin{aligned} \vec{q}_{2\perp} &= \vec{q}_l - \vec{q}_{1\perp}, \\ \vec{q}_{5\perp} &= -\vec{q}_{1\perp}, \end{aligned} \quad (2.21)$$

$$\begin{aligned} \vec{q}_{6\perp} &= \vec{q}_{1\perp} + \vec{q}_r, \\ \vec{q}_{7\perp} &= -\vec{q}_{4\perp}, \\ \vec{q}_{3\perp} &= -\vec{q}_{4\perp} - \vec{q}_l, \end{aligned} \quad (2.22)$$

$$\begin{aligned} \vec{q}_{8\perp} &= \vec{q}_{4\perp} - \vec{q}_r, \\ u_1 &= (q_5 + q_6)^2 = -M_{1\perp}^2 - q_r^2 - q_\perp^2 + 2d^2, \\ u_2 &= (q_7 + q_8)^2 = -M_{2\perp}^2 - q_r^2 - q_\perp^2 + 2d^2. \end{aligned} \quad (2.23)$$

In the amplitude all integrations run from  $-\infty$  to  $+\infty$ .

The particle-Reggeon vertices are analytic functions of the momentum transfers and the cluster mass. They possess poles in the  $\alpha$  and  $\beta$  complex plane from the propagators, whose position depends on the values of  $M^2$  and the  $l$ 's. At some particular value of  $M^2$  (say) two or more of the poles may pinch the hypercontour in the  $\alpha$ - $\beta$  plane, and the two-Reggeon-two-particle amplitude develops a singularity which corresponds to a slicing of the graph: Following Cutkosky, the discontinuity across the singularity is

calculated by replacing  $(q^2 - m^2 + i\epsilon)^{-1}$  by  $(-2\pi i)\delta^+(q^2 - m^2)$ . In addition, we will find generally that the pinching will only take place if either  $\alpha$  or  $\beta$ s or both is confined to a restricted range; for instance, the diffractive slicings, or discontinuities across the normal thresholds in the missing mass in the Reggeon-particle amplitudes, are present only for  $0 < \alpha_1 < 1$  so that in the equation for the discontinuity across that threshold the  $\alpha$  integration runs from zero to one only. The procedure which will be followed in determining the weight of a slicing (which is, of course, completely general and does not apply only to the Mandelstam graph) will be as follows:

(1) Draw a slicing in the graph which will separate the lines  $p_1$  and  $p_2$  from  $p_3$  and  $p_4$  while leaving  $p_1$  and  $p_2$ , and  $p_3$  and  $p_4$ , connected to each other.

(2) Look at the part of the amplitude composed of all the propagators which were sliced in step (1) and find if there is a pinch on the  $\alpha, \beta$  hypercontour; if so, learn what sort of a singularity in the external and internal variables it corresponds to, and what the ranges of integration on  $\alpha$  and  $\beta$  are, such that the pinch exists.

(3) Calculate the discontinuity across the singularity: place all the intermediate (sliced) particles on the mass shell and take the complex conjugate of the part of the amplitude to the right of the slice.

(4) If it is necessary to take a second discontinuity in one term in order to compare it to another, do so. In these calculations this case arises when the discontinuity of the amplitude has cuts in  $M^2$ . The  $M^2$  contour, which runs from  $-\infty$  to  $+\infty$ , is wrapped around its singularities in a manner analogous to techniques discussed by Rothe,<sup>9</sup> so that instead of integrating the function from  $M^2 = -\infty$  to  $\infty$  one integrates the discontinuity of the function along the branch cut. Note that since the  $\alpha, \beta$  integrations are now bounded, new singularities, not present in the amplitude, can be present in the sliced amplitude in the form of end-point singularities. These must also be taken into account in the contour rotation.

(5) Add all the discontinuities together to find the imaginary part of the scattering amplitude. From this expression the contribution to the total cross section can be found. Actually, it is well known that the contribution of the two-Pomeron cut to the total cross section is negative,<sup>2,4</sup> and the interesting part of this calculation lies in seeing how this result is obtained.

Step (1) must be guided by insight since there are obviously an infinite number of slicings which can be made. Arguments will be advanced to demonstrate why only the particular set of graphs discussed here are important.

## III. DIFFRACTIVE DISCONTINUITIES

The diffractive discontinuities are so named because they do not involve slicing any Reggeons. They correspond to the square of two-to-four production processes with a large rapidity gap, except that the lines are crossed. They are shown in Figs. 2(a) and 2(b). I will call the slice involving  $q_1$ ,  $q_2$ ,  $q_3$ , and  $q_4$  the " $M^2$  discontinuity" since

$$\int \frac{d\alpha_1 d(\beta_2 s) d\beta_3 d(\alpha_4 s)}{[\beta_3(M_{2\perp}^2 - \alpha_4 s) - \mu_3^2 + i\epsilon][(1 - \beta_3)\alpha_4 s - \mu_4^2 + i\epsilon]} \frac{1}{[\alpha_1(M_{1\perp}^2 - \beta_2 s) - \mu_1^2 + i\epsilon][(1 - \alpha_1)\beta_2 s - \mu_2^2 + i\epsilon]}. \quad (3.1)$$

The pinching in  $\alpha_1$  and  $\beta_3$  and  $\alpha_4$  happens separately and in an identical manner in each case (as can be seen by just relabeling variables in the first two propagators) and so it suffices to consider the pinching in  $B_1$  or  $B_2$  only.

In the amplitude  $B_1$ , the  $\alpha_1$  and  $\beta_2 s$  integrals run from  $-\infty$  to  $+\infty$ . Poles lie in the  $\alpha_1$  complex plane at

$$\alpha_1 = \frac{\mu_1^2 - i\epsilon}{M_{1\perp}^2 - \beta_2 s} \quad (3.2a)$$

and

$$1 - \alpha_1 = \frac{\mu_2^2 - i\epsilon}{\beta_2 s}. \quad (3.2b)$$

In order that a pinch between them can exist, one requires

$$(M_{1\perp}^2 - \beta_2 s) \beta_2 s > 0, \quad (3.3)$$

which is satisfied by

$$M_{1\perp}^2 > \beta_2 s > 0. \quad (3.4)$$

the pinching of lines  $q_1$  and  $q_2$  and  $q_3$  and  $q_4$  occur at the  $M^2$  normal thresholds of the amplitudes  $B_1$  and  $B_2$ . Similarly, the slice involving  $q_5$  and  $q_8$  will be called the " $u$  discontinuity." The  $M^2$  integration over the  $B$  functions are performed at fixed  $t$ , so right-hand cuts in  $u$  appear as left-hand cuts in  $M^2$ , and vice versa.

The  $M^2$  discontinuities arise from the pinching of the poles in the integrand

Then  $0 < \alpha_1 < \infty$  from (3.2a) and  $0 < 1 - \alpha_1 < \infty$  from (3.2b), so that a pinch is possible only if

$$0 < \alpha_1 < 1. \quad (3.5)$$

(This discussion assumes  $\mu_i^2 > 0$  for all  $i$ ; this is true as long as the  $q_i$  integration contour is not distorted too far from the real axis. The positivity of  $\mu_i^2$  will be assumed throughout the paper).

The contribution of this term to the imaginary part of the amplitude may now be cauculated by replacing the cut lines with  $\delta$  functions and taking complex the conjugate of the part of the amplitude to the right of the slice; i.e.,

$$2 \text{Im}A = \int d\Omega_n \prod_{j=1}^n [-2\pi i \delta(q_j^2 - m_j^2)] T_2^{(1)} T_2^{(2)*}, \quad (3.6)$$

with  $d\Omega_n$  being the phase-space integral over the intermediate on-mass-shell states. The  $M^2$  discontinuity of  $A$  is

$$\begin{aligned} 2 \text{Im}A(s, t) = & \frac{1}{(2\pi)^8} \int \frac{dt_1 dt_r}{\sqrt{-\lambda}} \theta(-\lambda) \int_{M_{1\perp}^2=0}^{\infty} dM_1^2 \int_{M_{2\perp}^2=0}^{\infty} dM_2^2 s^{\alpha_1 + \alpha_r - 1} \beta(t_1) \xi_i[\beta(t_r) \xi_r]^* \\ & \times \int_0^1 d\alpha_1 \int_0^{M_{1\perp}^2} d(\beta_2 s) \int_0^1 d\beta_3 \int_0^{M_{2\perp}^2} d(\alpha_4 s) \\ & \times \prod_{i=1}^4 \frac{[-2\pi i \delta(q_i^2 - m_i^2)] d^2 q_{1\perp} d^2 q_{4\perp} [(\alpha_1)(1 - \beta_3)]^{\alpha_r} [(1 - \alpha_1)\beta_3]^{\alpha_t}}{(q_5^2 - m_5^2 + i\epsilon)(q_6^2 - m_6^2 - i\epsilon)(q_7^2 - m_7^2 + i\epsilon)(q_8^2 - m_8^2 - i\epsilon)}. \end{aligned} \quad (3.7)$$

We now look more closely at the  $M^2$  discontinuity of  $B_1$  as formed by Eq. (3.6):

$$\begin{aligned} \text{disc}_{M_1^2} B_1 = & (-2\pi i)^2 \int_0^1 d\alpha_1 \int_0^{M_{1\perp}^2} d(\beta_2 s) d^2 q_{1\perp} (\alpha_1)^{\alpha_r} (1 - \alpha_1)^{\alpha_t} \\ & \times \frac{\delta(\alpha_1(M_{1\perp}^2 - \beta_2 s) - \mu_1^2) \delta((1 - \alpha_1)\beta_2 s - \mu_2^2)}{[-(1 - \alpha_1)(M_{1\perp}^2 - \beta_2 s - d^2) - \mu_5^2 + i\epsilon][-\alpha_1(\beta_2 s - d^2) - \mu_6^2 - i\epsilon]}. \end{aligned} \quad (3.8)$$

Performing the  $\beta_2 s$  integration over the second  $\delta$  function, we find

$$\text{disc}_{M_1^2} B_1 = (-2\pi i)^2 \int_0^1 d\alpha_1 d^2 q_{1\perp} \delta\left(M_{1\perp}^2 - \frac{\mu_1^2}{\alpha_1} - \frac{\mu_2^2}{1-\alpha_1}\right) \frac{(\alpha_1)^{\alpha_r} (1-\alpha_1)^{\alpha_l}}{[\alpha_1(1-\alpha_1)d^2 - \mu_1^2 + \alpha_1(\mu_1^2 - \mu_5^2) + i\epsilon]} \times \frac{1}{[\alpha_1(1-\alpha_1)d^2 - \mu_6^2 + d_1(\mu_6^2 - \mu_2^2) - i\epsilon]} \tag{3.9}$$

The discontinuity exists along the surface

$$M_{1\perp}^2 - \frac{\mu_1^2}{\alpha_1} - \frac{\mu_2^2}{1-\alpha_1} = 0 \tag{3.10}$$

and one finds [by minimizing  $\mu_1^2/\alpha_1 + \mu_2^2/(1-\alpha_1)$  with respect to  $\alpha_1$  and  $\vec{q}$ ] that this surface is a cut in the  $M_1^2$  plane with a branch point at

$$M_1^2 = (m_1 + m_2)^2 .$$

The act of slicing the Mandelstam graph along the line of Fig. 2(a) has resulted in taking the discontinuity of the box graphs  $B_1$  and  $B_2$  across their normal thresholds in the cluster mass.

The situation with the  $u$  discontinuities is similar. The pinch in  $B_1$  occurs between the other two poles,  $q_5$  and  $q_6$ , and one finds a pinch can happen only if  $d^2 > \beta_2 s > M_{1\perp}^2$  and  $0 < \alpha_1 < 1$ . The  $u$  discontinuity of  $B_1$  is

$$\text{disc}_{u_1} B_1 = (-2\pi i)^2 \int_0^1 d\alpha_1 d^2 q_{1\perp} \delta\left(M_{1\perp}^2 + \frac{\mu_s^2}{\alpha_1} + \frac{\mu_5^2}{1-\alpha_1}\right) \times \frac{(1-\alpha_1)^{\alpha_l} (\alpha_1)^{\alpha_r}}{[\alpha_1(1-\alpha_1)d^2 - \mu_1^2 - \alpha_1(\mu_5^2 - \mu_1^2) + i\epsilon][\alpha_1(1-\alpha_1)d^2 - \mu_2^2 + \alpha_1(\mu_2^2 - \mu_6^2) - i\epsilon]} \tag{3.11}$$

Again the singularity surface is a cut with a branch point at

$$M_1^2 = -(m_5 + m_6)^2 - q_r^2 - q_l^2 + 2d^2 .$$

This is the position of the  $u$ -channel normal threshold branch point in  $B$ .

Finally, let us calculate the contribution of the diffractive slices to the imaginary part of the two-to-two amplitude:

$$(2 \text{Im}A)_{\text{diff}} = \int \frac{dt_l dt_r \theta(-\lambda)}{\sqrt{-\lambda} 16(2\pi)^8} \beta(t_l)\beta(t_r) s^{\alpha_l + \alpha_r - 1} \left( \int_{M_{1\perp}^2=0}^{\infty} dM_1^2 \int_{M_{2\perp}^2=0}^{\infty} dM_2^2 \text{disc}_{M_1^2} B_1 \text{disc}_{M_2^2} B_2 \xi_l \xi_r^* + \int_{-M_{1\perp}^2=0}^{M_{1\perp}^2=0} dM_1^2 \int_{-M_{2\perp}^2=0}^{M_{2\perp}^2=0} dM_2^2 \text{disc}_{u_1} B_1 \text{disc}_{u_2} B_2 \xi_l^* \xi_r \right) \tag{3.12}$$

The amplitude  $B$  is closely related to the box graph if the Reggeons are treated as particles of mass  $t_l$  and  $t_r$  (compare Fig. 3), the only difference being the presence of the  $(1-\alpha_1)^{\alpha_l} (\alpha_1)^{\alpha_r}$  terms. These terms do not affect the  $M^2$  singularity structure of the amplitude. With the external masses  $m_1, m_2, t_l$ , and  $t_r$  small, the only singularities of the box graph in the  $M^2$  plane are left-

and right-hand normal threshold cuts. An integral of  $B$  along the contour shown in Fig. 4 will equal zero and so (since the function is sufficiently convergent that the infinite semicircles do not contribute)

$$\int_{M^2=4m^2}^{\infty} dM^2 \text{disc}_{M^2} B + \int_{u=4m^2}^{u=\infty} dM^2 \text{disc}_u B = 0 . \tag{3.13}$$

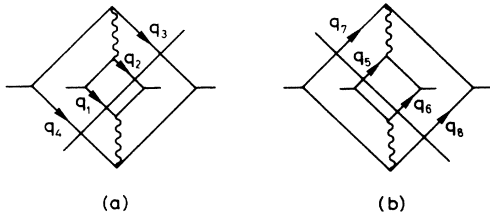


FIG. 2. Diffractive discontinuities: (a)  $M^2$  discontinuity; (b)  $u$  discontinuity.

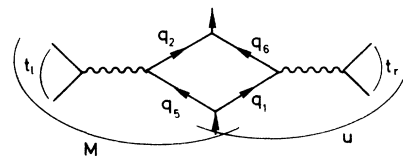


FIG. 3. The function  $B_1$ . The Reggeons shown here only represent the residual terms in the numerator of (2.17).

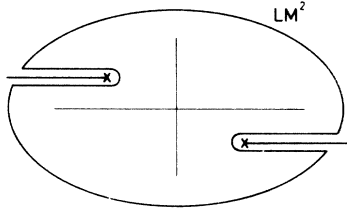


FIG. 4 Singularity structure of  $B_1$ , the two-particle—two-Reggeon vertex, in the  $M^2$  plane. The contour of integration leading to (3.13) is shown.

With the definition of the residue of the fixed pole at  $j = -1$

$$N_i(t, t_l, t_r) = \int_{\text{right-hand cut}} dM_i^2 \text{disc}_{M_i^2} B_i(M_i^2, t, t_l, t_r), \quad (3.14)$$

the diffractive contribution to the imaginary part of the amplitude may be written as

$$(2 \text{Im}A)_{\text{diff}} = \int \frac{dt_l dt_r \theta(-\lambda)}{16(2\pi)^8 \sqrt{-\lambda}} \beta(t_l) \beta(t_r) s^{\alpha_l + \alpha_r - 1} \times N_1(t, t_1, t_2) N_2(t, t_1, t_2) \times (\xi_l \xi_r^* + \xi_l^* \xi_r) \quad (3.15)$$

by combining the integrals of the left- and right-hand cuts in  $M^2$ . A technique due to Ref. 5 enables one to simplify the expression. The Reggeons are assumed to be simple poles of positive signature and may be written schematically as

$$\beta(t_i) \xi_i s_i^{\alpha_i} \rightarrow iD_i. \quad (3.16)$$

The two-Reggeon amplitude may be represented as

$$A(s, t) = -i(iD_l)(iD_r) \quad (3.17)$$

(all integrations and Reggeon-particle vertices have been dropped). Then the  $M^2$  and  $u$  slicings produce a Reggeon counting of

$$\text{Im}A = (iD_l)(iD_r)^* + (iD_l)^*(iD_r) = 2(\text{Im}D_l \text{Im}D_r + \text{Re}D_l \text{Re}D_r). \quad (3.18)$$

The overall factor of 2 is the weight with which the diffractive slicings contribute to  $\text{Im}A$ . Equation (3.18) written in a form similar to (3.15) is

$$(2 \text{Im}A)_{\text{diff}} = \int \frac{dt_l dt_r \theta(-\lambda)}{16(2\pi)^8 \sqrt{-\lambda}} s^{\alpha_r + \alpha_l - 1} \times N_1 N_2 [2(\text{Im} \xi_l \text{Im} \xi_r - \text{Re} \xi_l \text{Re} \xi_r)]. \quad (3.19)$$

IV. SLICING BOTH REGGEONS

We turn next to the slicing shown in Fig. 5—a cut down both Reggeons. The singularity structure of the two-particle—two-Reggeon vertex

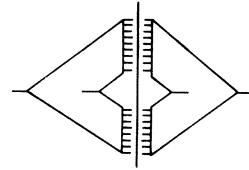


FIG. 5. Slicing through both Reggeons.

sliced in this manner is quite different from that of the unsliced vertex.

Of course, there are many cuts which slice one or both Reggeons only part way, as in Fig. 6. Such slicings in which the Reggeon is cut almost completely involve the production of a very large mass at the end of the Reggeon. They do not contribute with cutlike asymptotic behavior if one assumes that any amplitude in which a large  $q^2$  is carried on a virtual line is suppressed (cf. Ref. 5). In this case the line  $q$  decays into a mass comparable to  $s$  and so the contribution of such a slice is asymptotically small. (A  $q^2 \sim s$  is outside the range of usefulness of the Sudakov variables, for the longitudinal  $\delta$  functions no longer decouple: One would not expect Regge behavior for such a slicing since the rapidity gap across the Reggeon is small.) Slices which cut a small number of rungs (thinking of the Reggeon as a ladder) are just corrections to the diffractive discontinuity; they figure in the cancellation of the AFS (Amati-Fubini-Stanghellini) cut in planar diagrams.<sup>2,5</sup> Slices which cut a Reggeon completely in two are important since this sort of cutting can be done with the  $q^2$ 's small and since the discontinuity of a Reggeon amplitude is proportional to that amplitude.

In order to investigate the singularities resulting from the pinching of the two Reggeons, it is convenient to write the Reggeon amplitude in a dispersed form:

$$\xi_i s^{\alpha_i} = \frac{1}{-2\pi i} \int_0^\infty \frac{dm^2}{s - m^2 + i\epsilon} \text{disc}_{m^2} [\xi_i (m^2)^{\alpha_i}], \quad (4.1)$$

where

$$\text{disc}_{m^2} [\xi_i (m^2)^{\alpha_i}] = \text{disc}_{m^2} \left[ \frac{e^{i\pi\alpha_i}}{\sin\pi\alpha_i} (m^2)^{\alpha_i} \right] = -2i(m^2)^{\alpha_i}. \quad (4.2)$$

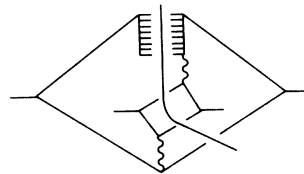


FIG. 6. A slicing which does not contribute to the cutlike behavior of  $A(s, t)$ .

The pinching may be sought between the denominators of the Reggeon dispersion relations. That is, it arises in the expression

$$\int d\alpha_1 d\beta_3 \frac{1}{[\alpha_1(1-\beta_3)s - m_r^2 + i\epsilon][(1-\alpha_1)\beta_3s - m_l^2 + i\epsilon]} \tag{4.3}$$

The  $\beta_3$  integral vanishes unless  $1 > \alpha_1 > 0$ , for only then does one pole lie in the  $\beta_3$  upper half plane and one pole in the lower half plane. When the pole in  $s'_1$  is encircled, the pinching expression becomes

$$R = \frac{1}{s} \int_0^1 \frac{d\alpha_1}{\alpha_1(1-\alpha_1)} \left( s - \frac{m_r^2}{\alpha_1} - \frac{m_l^2}{1-\alpha_1} + i\epsilon \right)^{-1} \tag{4.4}$$

Pinching arises along a branch cut in  $s$  whose branch point is given at the minimum of

$$s_0 = \frac{m_r^2}{\alpha_1} + \frac{m_l^2}{1-\alpha_1},$$

i.e., at

$$s_0 = (m_r + m_l)^2$$

(which is expected). Note that since the range of  $\alpha_1$  over which the integral is singular as  $0 < \alpha_1 < 1$ ,  $\beta_3$  is also confined to  $0 < \beta_3 < 1$ . The imaginary part of  $A$  resulting from this slice is

$$\begin{aligned} (2 \text{Im}A)_{\text{double abs}} &= \frac{1}{16(2\pi)^8 s} \int \frac{dt_l dt_r \theta(-\lambda)}{\sqrt{-\lambda}} dM_1^2 dM_2^2 \\ &\times \int \frac{dm_l^2}{2\pi i} \text{disc}_{m_l^2} [\beta(t_l) \xi_l(m_l^2)^{\alpha_l}] [-2\pi i \delta((1-\alpha_1)\beta_3s - m_l^2)] \\ &\times \int \frac{dm_r^2}{2\pi i} \text{disc}_{m_r^2} [\beta(t_r) \xi_r(m_r^2)^{\alpha_r}] [-2\pi i \delta(\alpha_1(1-\beta_3)s - m_r^2)] \\ &\times \int_0^1 d\alpha_1 \int_{-\infty}^{\infty} d(\beta_2s) d^2q_{1\perp} [(q_1^2 - m_1^2 + i\epsilon)(q_5^2 - m_5^2 + i\epsilon) \\ &\quad \times (q_2^2 - m_2^2 - i\epsilon)(q_6^2 - m_6^2 - i\epsilon)]^{-1} \\ &\times \int_0^1 d\beta_3 \int_{-\infty}^{\infty} d(\alpha_4s) d^2q_{4\perp} [(q_3^2 - m_3^2 + i\epsilon)(q_7^2 - m_7^2 + i\epsilon)(q_4^2 - m_4^2 - i\epsilon)(q_8^2 - m_8^2 - i\epsilon)]^{-1} \end{aligned} \tag{4.5}$$

The  $i\epsilon$  prescription for the propagators to the right of the slice is reversed because they are complex-conjugated.

After eliminating the  $\delta$  functions by doing the  $m_r^2$  and  $m_l^2$  integrations, we consider the cut  $B_1$ :

$$\begin{aligned} (\text{disc}_s B_1)_{\text{double abs}} &= \int_0^1 d\alpha_1 \int_{-\infty}^{\infty} \frac{d(\beta_2s) d^2q_{1\perp} (1-\alpha_1)^{\alpha_l} (\alpha_1)^{\alpha_r}}{\alpha_1(M_{1\perp}^2 - \beta_2s) - \mu_1^2 + i\epsilon} \\ &\times \frac{1}{[-(1-\alpha_1)(M_{1\perp}^2 - \beta_2s - d^2) - \mu_5^2 + i\epsilon][(1-\alpha_1)\beta_2s - \mu_2^2 - i\epsilon][-\alpha_1(\beta_2s - d^2) - \mu_6^2 - i\epsilon]} \end{aligned} \tag{4.6}$$

For  $0 < \alpha_1 < 1$  the complex  $\beta_2s$  plane has poles above the real axis due to  $q_1$  and  $q_2$  and in the lower half plane due to  $q_5$  and  $q_6$  (see Fig. 7). Since the contour of integration runs along the real axis, neither the  $q_1$  and  $q_2$ , nor the  $q_5$  and  $q_6$ , poles collide to pinch the hypercontour. A pinching of the first two poles would lead to a singularity corresponding to the normal threshold in  $M_1^2$  while a

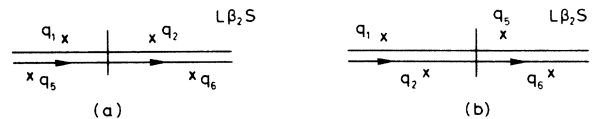


FIG. 7. Singularity structure of (a)  $(\text{disc}_s B_1)_{\text{double}}$ , and (b)  $B_1$  in the  $\beta_2s$  plane, for  $0 < \alpha_1 < 1$ , showing the integration contour.



pinching of the last two poles corresponds to the  $u$ -channel normal threshold. Such pinching occurs in the amplitude  $B$  when  $0 < \alpha < 1$ ; all the  $i\epsilon$ 's of (4.6) are positive and so the  $q_1$  and  $q_5$  poles lie in the upper half plane, the  $q_2$  and  $q_4$  poles in the lower half plane. We must therefore conclude that when the amplitude is sliced through both

Reggeons, the Reggeon-particle vertices possess no normal thresholds in the cluster mass.

To show the absence of normal thresholds explicitly (and to find out if some other singularities are present), close the  $\beta_2$ s contour about the  $q_1$  and  $q_2$  poles to give

$$\begin{aligned}
 (\text{disc}_s B_1)_{\text{double abs}} &= -2\pi i \int_0^1 \frac{d\alpha_1 d^2 q_{1\perp} (\alpha_1)^{\alpha_r - 2} (1 - \alpha_1)^{\alpha_r - 2}}{M_{1\perp}^2 - \mu_1^2 / \alpha_1 - \mu_2^2 / (1 - \alpha_1) - i\epsilon \sigma_{\alpha-1/2}} \\
 &\times \left\{ \frac{1}{M_{1\perp}^2 - d^2 - \mu_1^2 / \alpha_1 + \mu_6^2 / \alpha_1 + i\epsilon} \frac{1}{d^2 - \mu_1^2 / \alpha_1 - \mu_5^2 / (1 - \alpha_1) - i\epsilon} \right. \\
 &\quad \left. - \frac{1}{M_{1\perp}^2 - d^2 - \mu_2^2 / (1 - \alpha_1) + \mu_5^2 / (1 - \alpha_1) + i\epsilon} \frac{1}{d^2 - \mu_6^2 / \alpha_1 - \mu_2^2 / (1 - \alpha_1) - i\epsilon} \right\} \\
 &\quad (\sigma_x = x/|x|), \quad (4.7)
 \end{aligned}$$

which appears to have the 1-2 normal threshold pinch. By a little algebra the propagators may be arranged to give

$$\begin{aligned}
 (\text{disc}_s B_1)_{\text{double abs}} &= -2\pi i \int_0^1 \frac{d\alpha_1 d^2 q_{1\perp} (\alpha_1)^{\alpha_r} (1 - \alpha_1)^{\alpha_l}}{[\alpha_1 (M_{1\perp}^2 - d^2) - \mu_1^2 + \mu_6^2 + i\epsilon][ (1 - \alpha_1) (M_{1\perp}^2 - d^2) - \mu_2^2 + \mu_5^2 - i\epsilon]} \\
 &\times \left[ \frac{1}{-\alpha_1 (1 - \alpha_1) d^2 + \mu_1^2 + \alpha_1 (\mu_5^2 - \mu_1^2) - i\epsilon} - \frac{1}{-\alpha_1 (1 - \alpha_1) d^2 + \mu_6^2 + \alpha_1 (\mu_2^2 - \mu_6^2) + i\epsilon} \right], \quad (4.8)
 \end{aligned}$$

which obviously lacks the normal threshold singularity. However, if this function is integrated over  $M^2$  to find the fixed-pole residue, one sees that the  $M^2$  poles lie on either side of the  $M^2$  axis; therefore, wrapping the contour about one of them gives

$$\begin{aligned}
 \int_{-\infty}^{\infty} dM_1^2 \text{disc}_s B_1 &= (-2\pi i)^2 \int_{-\infty}^{\infty} dM_1^2 \delta \left( M_{1\perp}^2 - d^2 - \frac{\mu_1^2 - \mu_6^2}{\alpha_1} \right) d\alpha_1 d^2 q_{1\perp} (1 - \alpha_1)^{\alpha_l} (\alpha_1)^{\alpha_r} \\
 &\times \left[ \frac{1}{-\alpha_1 (1 - \alpha_1) d^2 + \mu_1^2 + \alpha_1 (\mu_5^2 - \mu_1^2) + i\epsilon} - \frac{1}{-\alpha_1 (1 - \alpha_1) d^2 + \mu_6^2 + \alpha_1 (\mu_2^2 - \mu_6^2) + i\epsilon} \right]. \quad (4.9)
 \end{aligned}$$

The  $M_1^2$  integral around the pole has been shown explicitly for comparison with (3.9). In both cases  $M_1^2$  has been removed from the integral everywhere except in the  $\delta$  function; integrating over the  $\delta$  function just eliminates it and the  $M^2$  integration from the expression for  $N$ . In both cases one finds

$$N = (-2\pi i)^2 \int_0^1 \frac{d\alpha_1 d^2 q_{1\perp} (\alpha_1)^{\alpha_r} (1 - \alpha_1)^{\alpha_l}}{-\alpha_1 (1 - \alpha_1) d^2 + \mu_1^2 + \alpha_1 (\mu_5^2 - \mu_1^2) - i\epsilon} \frac{1}{-\alpha_1 (1 - \alpha_1) d^2 + \mu_6^2 + \alpha_1 (\mu_2^2 - \mu_6^2) + i\epsilon}. \quad (4.10)$$

The contribution of this slicing to the cut can be found by using the trick of Ref. 5: Slicing a Reggeon effectively changes the signature from  $\xi$  to  $2i \text{Im} \xi$ . In addition, there is a factor of  $i$  from the closed loop on either side of the slice (see Fig. 5), and so the slicings through no and two Reggeons combine to give

$$\begin{aligned}
 2 \text{Im} A &= \int \frac{dt_l dt_r \theta(-\lambda)}{\sqrt{-\lambda}} N_1 N_2 s^{\alpha_l + \alpha_r - 1} \\
 &\times (2 \text{Im} \xi_r \text{Im} \xi_l - 2 \text{Re} \xi_l \text{Re} \xi_r + 4 \text{Im} \xi_l \text{Im} \xi_r), \quad (4.11)
 \end{aligned}$$

which is still positive-definite.

It is remarkable that two functions which have such different behavior in the  $M^2$  plane should give identical answers upon integration over  $M^2$ , and it is of some interest to investigate further to see where this result comes from.

First of all, the phase space of the internal loop momenta is bounded by the pinch requirement. This boundedness introduces end-point singularities which are easily seen in the last two denominators of (4.8), at  $\alpha = 0$  and  $\alpha = 1$ . In the denominator

$$\alpha_1(M_{1\perp}^2 - d^2) - \mu_1^2 + \mu_6^2 + i\epsilon,$$

for instance, an  $\alpha_1 = 0$  end-point singularity is found at  $M_{1\perp} = \infty$  and an  $\alpha_1 = 1$  end-point singularity at

$$M_{1\perp}^2 = d^2 + \mu_1^2 - \mu_6^2 - i\epsilon. \quad (4.12)$$

The branch points of this singularity lie at the minima of (4.12) with respect to  $q_{\perp}$ . But writing  $\mu_1^2 = q_{\perp}^2 + m_1^2$ ,  $\mu_6^2 = (q_{\perp} + k)^2 + m_6^2$ , we see (4.12) has no minimum in  $q_{\perp}$ . This cut runs from  $-\infty$  to  $\infty$  in the  $M^2$  plane. For the sake of simplicity the branch line may be distorted into a semicircle at infinity. Then, since the function is sufficiently convergent at infinity (it vanishes like  $M_1^{-4}$ ), this cut will give no contribution to the integral when the  $M^2$  contour rotation is performed. The same argument holds, of course, for the last denominator of (4.8).

Other singularities may result from the pinching of three propagators on the hypercontour [as can be seen from Fig. 7(a)]. For instance, the first and third denominators of (4.8) may pinch. Then one requires

$$\begin{aligned} -\alpha_1(1 - \alpha_1)d^2 + \mu_1^2 + \alpha_1(\mu_5^2 - \mu_1^2) - i\epsilon &= 0, \\ \alpha_1(M_{1\perp}^2 - d^2) - \mu_1^2 + \mu_6^2 + i\epsilon &= 0 \end{aligned} \quad (4.13)$$

and the branch point in  $M^2$  may be found by minimizing these expressions with respect to  $\alpha$  and  $q$ .

But it is unnecessary to perform this calculation. Equation (4.13) is actually the set of equations

$$\begin{aligned} \alpha_1(M_{1\perp}^2 - \beta_2 s) - \mu_1^2 + i\epsilon &= 0, \\ -(1 - \alpha_1)(M_{1\perp}^2 - \beta_2 s - d^2) - \mu_5^2 + i\epsilon &= 0, \\ -\alpha_1(\beta_2 s - d^2) - \mu_6^2 + i\epsilon &= 0 \end{aligned} \quad (4.14)$$

from which  $\beta_2 s$  has been eliminated, which is to be minimized with respect to  $\alpha_1$ ,  $\beta_2 s$ , and  $q_1$ . A direct calculation is not the simplest way to proceed. One can write the integral (4.6) symbolically as

$$N = \int dM^2 \int \frac{d^4 k}{\prod_i (q_i^2 - m_i^2)}, \quad i = 1, 2, 5, 6$$

and introduce Feynman variables  $\lambda_i$  to write

$$N = \int dM^2 \int d^4 k \frac{\prod_i d\lambda_i \delta(1 - \sum \lambda_i)}{[\sum \lambda_i (q_i^2 - m_i^2)]^4}. \quad (4.15)$$

Then the singularity (4.14) occurs at

$$\begin{aligned} \lambda_2 &= 0, \\ q_i^2 - m_i^2 &= 0, \quad i = 1, 5, 6 \end{aligned}$$

and a minimization of the denominator of (4.15) with respect to  $k$  gives

$$\sum \lambda_i q_i = 0, \quad i = 1, 5, 6$$

which is the usual Landau equation for the triangle singularity of lines 1, 5, and 6.<sup>10</sup> The other three triangle singularities of the box graph arise from the other three combinations of three propagators in (4.8). If all propagators are required to pinch at the same point, the  $M^2$ - $u$  double-spectral function results.

The plausibility of this behavior is evident upon examination of Fig. 7(a): One sees that, even though the  $i\epsilon$  prescription is mixed, the higher-order Landau singularities still occur since the  $\beta_2 s$  contour is still trapped by them. Of course, the Landau equations tell only that singularities collide and not that a pinch results, but they can be used to tell where a pinch which is known to exist can be found.

It is also striking that the triangle singularities should appear on the physical sheet. This comes about when the cuts arising from the end-point singularities are moved from the finite  $M^2$  region to infinity. In the beginning they lie along the  $M^2$  real axis from  $-\infty$  to  $\infty$ . Then they are pushed back into infinite semicircles. But this distortion exposes the triangle singularities (and the box singularity) lying at complex  $M^2$ . Then the  $M^2$  integration is done. The end-point cuts at infinity do not contribute because the amplitude vanishes there; the integral around the higher-order Landau singularities reproduces the effect of the normal threshold.

## V. ABSORPTIVE CORRECTIONS

We turn now to the slicings which will reverse the sign of  $\text{Im}A$  given in Sec. III, those in which one Reggeon is cut completely. These slicings are shown in Fig. 8. They correspond to production processes in which a multiperipheral chain is produced and in which a Reggeon is exchanged internally between points at the top and bottom of the chain.

The analysis will be carried out along the lines of the previous two sections; the singularity structure in the  $M^2$  plane resulting from these slicings turns out (not unexpectedly) to be of an intermedi-

ate nature compared to the two cases of slicing no Reggeons or two Reggeons.

Writing the Reggeons via dispersion relations as in (4.1) we see the cutting of Fig. 8(a) takes place when the poles in

$$R = \int \frac{d\alpha_1 d(\beta_2 s) d\beta_3 d(\beta_4 s)}{[s_r - m_r^2 + i\epsilon][(1 - \alpha_1)\beta_2 s - \mu_2^2 + i\epsilon]} \times \frac{1}{\beta_3(M_{2\perp}^2 - \alpha_4 s - d^2) - \mu_3^2 + i\epsilon}, \quad (5.1)$$

with  $s_r = \alpha_1(1 - \beta_3)s$ , collide. The pinching, and its constraints on the phase space, may be investigated by evaluating the integrals one at a time.

Singularities lie in the  $\alpha_1$  plane at

$$\alpha_1 = \frac{m_r^2 - i\epsilon}{(1 - \beta_3)s}, \quad (5.2a)$$

$$1 - \alpha_1 = \frac{\mu_2^2 - i\epsilon}{\beta_2 s}. \quad (5.2b)$$

Only if  $(1 - \beta_3)\beta_2 > 0$  do the poles lie on the opposite sides of the  $\alpha_1$  contour so that pinching occurs. Assume that the inequality is satisfied and encircle the singularity (5.2b); then

$$R = 2\pi i \int \frac{d(\alpha_4 s) d\beta_3 d(\beta_2 s)}{\beta_2 s [(1 - (\mu_2^2 - i\epsilon)/\beta_2 s)(1 - \beta_3)s - m_r^2 + i\epsilon]} \times \frac{1}{\beta_3(M_{2\perp}^2 - \alpha_4 s - d^2) - \mu_3^2 + i\epsilon}. \quad (5.3)$$

The singularities in  $\beta_3$  lie at

$$\beta_3 = \frac{\mu_3^2 - i\epsilon}{M_{2\perp}^2 - \alpha_4 s - d^2} \quad (5.4)$$

and at

$$(1 - \beta_3)s = \frac{\beta_2 s(m_r^2 - i\epsilon)}{\beta_2 s - \mu_2^2 + i\epsilon} \quad (5.5)$$

$$= \frac{\beta_2 s m_r^2}{\beta_2 s - \mu_2^2} - i\epsilon \frac{\beta_2 s(m_r^2 + \beta_2 s - \mu_2^2)}{(\beta_2 s - \mu_2^2)^2} \quad (5.6)$$

$$= \frac{\beta_2 s m_r^2}{\beta_2 s - \mu_2^2} - i\epsilon \operatorname{sgn} \beta_2 s (m_r^2 + \beta_2 s - \mu_2^2), \quad (5.7)$$

where  $\operatorname{sgn}(x) \equiv x/|x|$ . The  $\epsilon$  in the denominator of (5.5) must be raised to the numerator in order that

$$(2 \operatorname{Im} A)_{\text{abs}} = \frac{(-2\pi i)^3}{16(2\pi)^8} \int \frac{dt_1 dt_r \theta(-\lambda)}{\sqrt{-\lambda}} \int dM_1^2 dM_2^2 \int_0^1 d\alpha_1 \int_0^\infty d(\beta_2 s) \int_0^1 d\beta_3 \int_{M_{2\perp}^2 - d^2}^\infty d(\alpha_4 s) \times \int \frac{dm_r^2}{-2\pi i} \operatorname{disc}_{m_r^2} [\xi_r(m_r^2)^{\alpha_r}] \delta(\alpha_1(1 - \beta_3)s - m_r^2) \beta(t_r) \beta(t_1) \xi_i s_i^{\alpha_i} \times \frac{\delta(\beta_3(M_{2\perp}^2 - \alpha_4 s - d^2) - \mu_3^2) \delta((1 - \alpha_1)\beta_2 s - \mu_2^2)}{\prod_{1,3,5,7} (q_i^2 - m_i^2 + i\epsilon) \prod_{6,8} (q_j^2 - m_j^2 - i\epsilon)}. \quad (5.10)$$

The first  $\delta$  function can easily be eliminated by doing the  $m_r^2$  integration. The heart of the calculation of

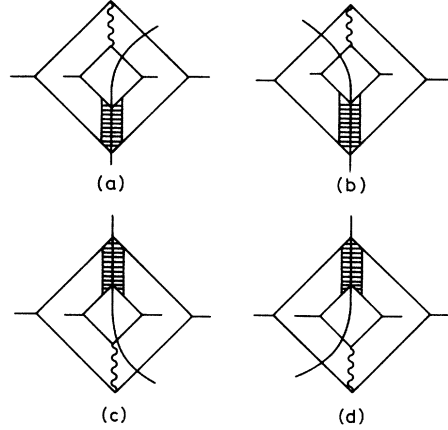


FIG. 8. Absorptive slicings of the Mandelstam graph.

the position of the pole in the complex plane can be determined. This is done by expanding the denominator ( $\epsilon$  is, after all, infinitesimal) and combining the  $O(\epsilon)$  term from the expansion with the  $\epsilon$  in the numerator. The only effect of the terms multiplying  $\epsilon$  is to determine its sign, and so the denominator is dropped in going from (5.6) to (5.7).

Now the phase-space constraints may be established: First, the only pinching solution to (5.2) is that  $\beta_2 > 0$ ,  $1 - \beta_3 > 0$ , and  $0 < \alpha_1 < 1$ . For a pinch in the  $\beta_3$  plane, either

$$-d^2 + M_{2\perp}^2 - \alpha_4 s > 0, \quad (5.8)$$

$$\beta_2 s - \mu_2^2 + m_r^2 > 0$$

and  $\beta_3 > 0$  from (5.4), so  $1 > \beta_3 > 0$ , or

$$-d^2 + M_{2\perp}^2 - \alpha_4 s < 0, \quad (5.9)$$

$$\beta_2 s - \mu_2^2 + m_r^2 < 0.$$

This second case can be excluded by recalling that if  $0 < \alpha_1 < 1$ , the second denominator of (5.1) will not vanish unless  $\beta_2 s > M_2^2$ , which is assumed to be a positive number.

The discontinuity of the amplitude in  $s$  along this slicing is found in a manner identical to that of the last two sections:

the discontinuity is to be found in the integral over the inner box,

$$\begin{aligned}
 (\text{disc}_s B_1)_{\text{abs}} = & -2\pi i \int_0^1 d\alpha_1 \int \frac{d(\beta_2 s)(\alpha_1)^{\alpha_1} r(1-\alpha_1)^{\alpha_1} \delta((1-\alpha_1)\beta_2 s - \mu_2^2)}{[\alpha_1(M_{1\perp}^2 - \beta_2 s) - \mu_1^2 + i\epsilon][-(1-\alpha_1)(M_{1\perp}^2 - \beta_2 s - d^2) - \mu_5^2 - i\epsilon]} \\
 & \times \frac{1}{[-\alpha_1(\beta_2 s - d^2) - \mu_6^2 - i\epsilon]}, \tag{5.11}
 \end{aligned}$$

and the outer box,

$$\begin{aligned}
 (\text{disc}_s B_2)_{\text{abs}} = & -2\pi i \int_0^1 d\beta_3 \int \frac{d(\alpha_4 s)d^2 q_{4\perp} (1-\beta_3)^{\alpha_4} r(\beta_3)^{\alpha_4} \delta(\beta_3(M_{2\perp}^2 - \alpha_4 s - d^2) - \mu_3^2)}{[-\beta_3(\alpha_4 s - d^2) - \mu_2^2 + i\epsilon][(1-\beta_3)\alpha_4 s - \mu_4^2 + i\epsilon]} \\
 & \times \frac{1}{[-(1-\beta_3)(M_{2\perp}^2 - \alpha_4 s) - \mu_8^2 - i\epsilon]}. \tag{5.12}
 \end{aligned}$$

The  $\beta_2$  integration may be used to eliminate the  $\delta$  function in (5.11):

$$\begin{aligned}
 (\text{disc}_s B_1)_{\text{abs}} = & -2\pi i \int_0^1 \frac{d\alpha_1 d^2 q_{1\perp} (\alpha_1)^{\alpha_1} r^{-1} (1-\alpha_1)^{\alpha_1}}{[M_{1\perp}^2 - \mu_2^2 / (1-\alpha_1) - \mu_1^2 / \alpha_1 + i\epsilon][-(1-\alpha_1)(M_{1\perp}^2 - d^2) + \mu_2^2 - \mu_5^2 + i\epsilon]} \\
 & \times \frac{1}{[-\mu_6^2 + \alpha_1(\mu_6^2 - \mu_2^2) + \alpha_1(1-\alpha_1)d^2 - i\epsilon]}. \tag{5.13}
 \end{aligned}$$

The first pole in the expression demonstrates that  $\text{disc}_s B_1$  has a normal threshold cut in  $M_1^2$ : Whenever  $M_{1\perp}^2 = (\mu_1 + \mu_2)^2$  two singularities pinch the  $\alpha_1$  contour at  $\alpha_1 = \mu_1 / (\mu_1 + \mu_2)$ ; i.e., anywhere in the range  $0 < \alpha_1 < 1$ . The other two propagators may simultaneously vanish at

$$M_{1\perp}^2 + \frac{\mu_5^2}{1-\alpha_1} + \frac{\mu_6^2}{\alpha_1} + 2d^2 - i\epsilon = 0,$$

but this pinching takes place at

$$\alpha_1 = \frac{d^2 + \mu_6^2 - \mu_2^2 \pm \lambda^{1/2}(d^2, \mu_6^2, \mu_2^2)}{2d^2},$$

i.e., for  $\alpha_1 > 1$  or  $\alpha_1 < 0$ , if  $d^2 < 4m^2$ . Therefore  $\text{disc}_s B$  has only a right-hand normal threshold in

$M_1^2$ .

However, the normal threshold is not the only singularity of  $\text{disc}_s B$  in  $M$ . We see in fact that the second propagator of (5.13) has a pole in the  $M$  upper half plane, while the normal threshold lies in the lower half plane. This singularity is "half" of the ones encountered in the slicing of both Reggeons: It is a combination of  $\alpha = 0$  end-point singularity (the  $\alpha = 1$  singularity lies at  $M^2 = \infty$ ) and, in conjunction with the third propagator, a triangle singularity between  $q_2$ ,  $q_5$ , and  $q_6$ . Therefore, when an  $M^2$  contour wrapping is performed to compare  $\int \text{disc}_s B dM^2$  with  $\int \text{disc}_{M^2} B dM^2$ , one can enclose either the normal threshold or the triangle-end-point singularity. The result is the same:

$$\begin{aligned}
 \text{disc}_{M^2} \text{disc}_s B_1 = & (-2\pi i)^2 \int_0^1 \frac{d\alpha_1 d^2 q_{1\perp} \delta(M_{1\perp}^2 - \mu_1^2 / \alpha_1 - \mu_2^2 / (1-\alpha_1)) (1-\alpha_1)^{\alpha_1} r^{-1} (\alpha_1)^{\alpha_1}}{[d^2 \alpha_1 (1-\alpha_1) - \mu_6^2 + \alpha_1(\mu_6^2 - \mu_2^2) - i\epsilon][-(1-\alpha_1)(M_{1\perp}^2 - d^2) + \mu_2^2 - \mu_5^2 + i\epsilon]} \\
 = & \text{disc}_{M^2} B. \tag{5.14}
 \end{aligned}$$

The situation in the outer box is identical. The integration over  $\alpha_4 s$  can be performed to eliminate the  $\delta$  function and then an expression identical to (5.13) results (except for a relabeling of all the variables) which has only a right-hand cut in  $M_2^2$  and, in addition, higher-order Landau singularities and end-point pinches which lie on the opposite side of the  $M^2$  contour from the normal threshold. Performing the  $M^2$  integration about either singularity gives a result of  $N_2$ . The contribution of Fig. 8(a) is, putting all the pieces together,

$$\begin{aligned}
 (2 \text{Im} A)_{\text{abs}} = & \int \frac{dt_1 dt_r \theta(-\lambda)}{16(2\pi)^8 \sqrt{-\lambda}} s^{\alpha_1 + \alpha_r - 1} N_1 N_2 \\
 & \times \xi_t \xi_r(-2), \tag{5.15}
 \end{aligned}$$

where the  $(-2)$  comes from the slicing of the Reggeon.

Calculation of the discontinuities from other graphs of Fig. 8 is carried out along lines similar to those just described. In each case, when the ranges of integration which are allowed for pinch-

ing are calculated, it will be found that the variables  $\alpha_1$  or  $\beta_3$  will range from 0 to 1, so that  $\text{disc}_s B$  will have only right-hand or only left-hand normal thresholds in  $M^2$  and, in addition, a com-

bination of end-point and triangle singularities.

For example, the slicing of Fig. 8(c) results from the pinching of the propagators

$$\int \frac{d\alpha_1 d(\beta_2 s) d\beta_3 d(\alpha_4 s)}{[(1-\alpha_1)\beta_3 s - m_1^2 + i\epsilon][-\alpha_1(\beta_2 s - d^2) - \mu_6^2 + i\epsilon][-(1-\beta_3)(M_{2\perp}^2 - \alpha_4 s) - \mu_8^2 + i\epsilon]} \quad (5.16)$$

Comparison with Eq. (5.1) shows that the transformations

$$\alpha_1 \rightarrow 1 - \alpha_1, \quad (5.17)$$

$$\beta_3 \rightarrow 1 - \beta_3, \quad \beta_2 s \rightarrow -(\beta_2 s - d^2), \quad (5.18)$$

$$M_{2\perp}^2 - \alpha_4 s - d^2 \rightarrow -(M_{2\perp}^2 - \alpha_4 s) \quad (5.19)$$

convert (5.1) into (5.16), so that the weight of this slice is identical to that of (5.14).

Since all the various discontinuities of the Reggeon-particle vertices enter with the same weight, one can again use the Reggeon-counting scheme of Ref. 5 to see how the absorptive slices contribute to the imaginary part. The slicings of Figs. 8(a)–8(d) give respectively

$$\begin{aligned} (2 \text{Im} A)_{\text{abs}} &= N_1 N_2 [(iD_1)(-i\delta D_r) + (iD_1)^*(-i\delta D_r) + (i\delta D_1)(iD_r) + (i\delta D_1)(iD_r)^*] \\ &= -8N_1 N_2 \text{Im} D_1 \text{Im} D_r, \end{aligned} \quad (5.20)$$

where  $\delta D = 2i \text{Im} D$  is the discontinuity in  $s$  of a Reggeon. The imaginary part of the two-to-two amplitude resulting from a sum of the diffractive, absorptive, and double-Reggeon slice imaginary parts is

$$\begin{aligned} 2 \text{Im} A &= 2N_1 N_2 (-\text{Im} D_1 \text{Im} D_r + \text{Re} D_1 \text{Re} D_r) \\ &= -2 \int \frac{dt_1 dt_r \theta(-\lambda)}{16(2\pi)^8 \sqrt{-\lambda}} N_1(t, t_1, t_r) N_2(t, t_1, t_r) \beta(t_1) \beta(t_r) s^{\alpha_1 + \alpha_r - 1} (\text{Im} \xi_1 \text{Im} \xi_r - \text{Re} \xi_1 \text{Re} \xi_r). \end{aligned} \quad (5.21)$$

If the Reggeons are nearly pure imaginary ( $\text{Re} \xi \approx 0$ ), then the one-Reggeon absorptive corrections reverse the sign of the diffractive discontinuity of  $A(s, t)$ .

## VI. GENERALITY OF THE RESULT

How general is this result? Does it apply to all field-theoretic vertices? Abramovskii, Kancheli, and Gribov<sup>5</sup> present arguments that any two-particle,  $\nu$ -Reggeon vertex should be unaffected by different slicings. In our language, they write such a vertex (Fig. 9) as

$$\begin{aligned} N_\nu &= \int_{-\infty}^{\infty} \prod_{i=1}^{\nu} \frac{d\alpha_i d\bar{\alpha}_i}{Z_i \bar{Z}_i} \delta(\sum \alpha_i + \sum \bar{\alpha}_i) \\ &\quad \times \prod_{i=1}^{\nu} d(\beta_i s) d(\bar{\beta}_i s) (\alpha_i)^{\alpha(\bar{t}_i)} d^2 q_{i\perp} R, \end{aligned} \quad (6.1)$$

where

$$Z_i = p_i^2 - m_i^2 + i\epsilon, \quad \bar{Z}_i = k_i^2 - m_i^2 + i\epsilon$$

and  $R$  is the  $(2\nu + 2)$ -particle blob. The cut vertex in which  $\mu$  of the  $\nu$  Reggeons are sliced,  $\mu_1$  are on the left-hand side of the cut, and  $\mu_2$  are on the right-hand side, is

$$\begin{aligned} N_{\nu}^{\mu_1, \mu_2} &= \int_0^{\infty} d\gamma \delta(\gamma - (\beta + \beta_1)) \\ &\quad \times \int_{-\infty}^{\infty} \prod_{i=1}^{\nu} \frac{d\alpha_i d\bar{\alpha}_i}{Z_i \bar{Z}_i} \delta(\sum \alpha_i + \sum \bar{\alpha}_i) \\ &\quad \times \prod d(\beta_i s) d(\bar{\beta}_i s) (\alpha_i)^{\alpha(\bar{t}_i)} d^2 q_{i\perp} \text{Abs}_W R, \end{aligned} \quad (6.2)$$

where  $\text{Abs}_W R$  is the absorptive part of  $R$  in the variable  $W = \gamma s$ . But, they say, this is the same as  $N$ : Equation (6.1) may be premultiplied by

$$\int_{-\infty}^{\infty} d\gamma \delta(\gamma - (\beta + \beta_2)) \quad (6.3)$$

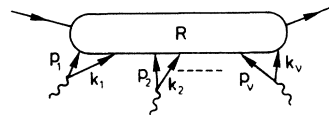


FIG. 9. A two-particle- $\nu$ -Reggeon vertex examined by Ref. 5 in the study of slicings of multi-Reggeon graphs.

and the contour of integration over  $\gamma$  distorted about the right-hand cut in  $R$ . Therefore Eq. (6.2) equals Eq. (6.1).

The arguments do not work for the following reasons: When the cut is made, some propagators  $Z_i$  or  $\bar{Z}_i$  find themselves to the left of the cut and their  $+i\epsilon$ 's change to  $-i\epsilon$ 's. This changes the analytic structure of the integral and quite different behavior may occur in  $N_v^{\mu, \mu_1, \mu_2}$ . Also, the limits of integration in  $\alpha_i$  and  $\bar{\alpha}_i$  are not always  $-\infty$  to  $\infty$ . The pinching of the singularities in the  $Z_i$ 's and in  $R$  which produce a normal threshold occur only for some limited range of the integration variables, which might be different in different slicings.

The contour distortion in  $\gamma$  going from (6.1) to

$$\int BdM^2 = \int d\alpha_1 (1 - \alpha_1)^{\alpha_1} (\alpha_1)^{\alpha_2} d^2 q_{1\perp} \times \int \frac{d(\beta_1 s)}{(\alpha_1 \beta_1 s - \mu_1^2 + i\epsilon) [-(1 - \alpha_1) \beta_1 s - \mu_5^2 + i\epsilon]} \int \frac{d(\beta_2 s)}{[(1 - \alpha_1) \beta_2 s - \mu_2^2 + i\epsilon] (-\alpha_1 \beta_2 s - \mu_6^2 + i\epsilon)}. \tag{6.4}$$

The amplitude has poles in  $\beta_1$  and  $\beta_2$  which lie on opposite sides of their contours for  $0 < \alpha_1 < 1$  only. This constraint is at least as strong as any constraint arising from a pinching in the diagram. Then, taking a slice of the Mandelstam graph converts at most one of the propagators in each  $\beta$  integral into a  $\delta$  function, possibly flipping the  $i\epsilon$  of the other propagator, or flips neither or both  $i\epsilon$ 's (but never just one alone). But all these operations leave the quantity  $\int f(\beta) d\beta$  unchanged.

Now if one follows a completely field-theoretic program and builds one's Reggeons out of ladders with  $n$  rungs, so that

$$\text{Reggeon} = \sum_{n=0}^{\infty} \frac{g^2 K^n(t) (\ln s)^n}{sn!},$$

and studies the exchange of such ladders, summing over  $n$  at the end of the calculation, one is justified in ignoring two-particle-two-Reggeon vertices which are more complicated than the Mandelstam graph. This is because detailed calculations of these scattering amplitudes show that their energy dependence is damped by powers of  $\ln s$  relative to the Mandelstam graph.<sup>11,12</sup>

These calculations have been also carried out for two-particle- $n$ -Reggeon amplitudes; a "nesting hypothesis"<sup>12</sup> has been proposed where the leading  $\ln s$  contribution to many-tower exchange is dominated by the generalized Mandelstam graphs shown in Figs. 10(a)–10(c). But all slices of these graphs leave  $N$  unchanged, as the following argument shows.

(6.2) may encounter singularities other than the one enclosed in (6.2) so that (6.1) and (6.2) differ by integrals along these other singularities. The singularity structure of  $B$  in the  $M^2$  plane can be—and as we have seen, is—generally quite different from the singularity structure of a discontinuity of  $B$ .

Despite these objections, the fact still remains that all the slicings of the Mandelstam graph give the same result. This happens because of the great symmetry of the amplitude, which is masked when the singularity structure of the vertex is studied as a function of  $M^2$ . For if the vertex is written as an integral over  $\beta_1$  and  $\beta_2$ , not  $\beta_2$  and  $M_1^2$ , it has the form (setting  $d^2 = 0$  for convenience)

Consider the three-Reggeon cut of figure 10(b) (with its labeling of lines). The inner two-Reggeon cut ( $R_2, R_3$ ) is made of  $\beta$  integrals identical to those in (6.4), with the exception that  $\alpha_1 + \alpha_5 = \alpha_0$ , not 1 as in (6.4). But one needs  $0 < \alpha_0 < 1$  so that the outer Mandelstam box does not vanish, so that the poles in all the  $\beta$  integrals are aligned as they are in (6.4). All slicings of the inner cut graph have the same weight; then, in studying the outer box one can replace the internal two-Reggeon cut

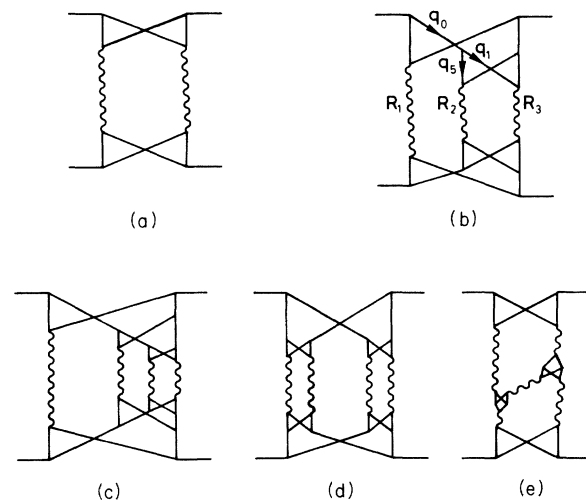


FIG. 10. (a)–(c) Multi-Reggeon cut graphs from the "nesting hypothesis." (d)–(e) Other multi-Reggeon cuts whose slicings obey the rules of Ref. 5.

by a "black box" four-point function: this reduces the problem to that of an ordinary Mandelstam graph, all of whose slicings have the same weight. The argument may be generalized to any sort of multi-Reggeon graph whose vertices are Mandelstam boxes or nests [Figs. 10(d) and 10(e)]. All slicings leave the various  $N$ 's unchanged.

The Reggeon calculus in its original formulation by Gribov<sup>13</sup> uses the Mandelstam vertex as its model for the two-Reggeon-two-particle vertex. No explicit picture of a two-particle- $n$ -Reggeon coupling is given. However, if the "nesting assumption" is used to construct these couplings, the resulting Reggeon calculus will satisfy all the slicing rules in Ref. 5. If one treats the Reggeons as ladders in weakly-coupled  $\phi^3$  theory and takes as the Reggeon-particle couplings a sum of Mandelstam graphs plus more complicated terms, these counting rules are correct in the dominant part of the multi-Reggeon graph but may be violated in the next-to-leading order of the amplitude.

Unfortunately, the ladder assumption which produces this counting can generate in  $\phi^3$  theory only a singularity at  $j = -1 + O(g^2)$  at  $t = 0$ . The singularity may be raised to  $j = 1$  if vector particles are exchanged. However, a result which is true only for a restricted class of perturbation-theory graphs (the slicing rules) is questionable if the coupling constant becomes large (as is the case in hadronic physics). We turn to another class of vertices, which evade this last problem and whose structure is rather different from field theory, as an input in the construction of a Reggeon calculus.

## VII. MULTI-REGGE AMPLITUDES AND VERTICES

So far in the discussion of Regge cuts no use has been made of our knowledge of Reggeon-particle vertices from another source: multi-Regge expansions of  $n$ -point functions. It would seem to be a natural extension, in the calculation of Regge-cut amplitudes from pole amplitudes whose analytic behavior is well understood, that one takes the vertices of the cut amplitude also to be closely related to vertices whose behavior can be studied in a more controlled environment. Indeed, the only way one has to compare Reggeon-cut contributions to pole contributions in the scattering amplitude is to assume that one can obtain the vertices of the cut from inclusive reactions and then perform the phase-space integrals. Such a program was first discussed by Muzinich, Paige, Trueman, and Wang,<sup>14</sup> and has recently been applied to the Reggeon calculus by Capella and Kaplan.<sup>15</sup>

The relevant vertex for the two-Reggeon cut is

shown in Fig. 11. It is a function of the variables

$$\begin{aligned} M^2 &= (p_2 + p_3 + p_4)^2, \\ u &= (p_3 + p_4 + p_5)^2, \\ S &= (p_1 + p_2 + p_3)^2, \\ s_{ij} &= (p_i + p_j)^2, \\ t_1 &= (p_1 + p_6)^2, \\ t_2 &= (p_3 + p_4)^2, \\ t &= (p_2 + p_5)^2, \end{aligned} \quad (7.1)$$

evaluated in the helicity limit

$$\begin{aligned} S &= s_{12} + s_{23}, \\ s_{12} &= s_{23} = s_{45} = s_{56} = s, \\ s &\rightarrow \infty, \quad M^2, t, t_1, t_2 \text{ fixed.} \end{aligned} \quad (7.2)$$

One can imagine building the two-Reggeon cut by taking two of these six-point functions, amputating the Reggeons on one of them, and gluing them together. (The alternate method of gluing them together as they stand is not done because if the Reggeons were ladders, joining the ladders and then summing over the rungs could lead to double counting.) The amplitude as it is drawn is planar in the sense that if it were a dual model, it would be planar with this particular ordering of external lines.

At this point it is necessary to make assumptions about the analytic properties of the six-point function. This is because our knowledge of the nature of higher-order Landau singularities is very incomplete and so, to get anywhere, assumptions must replace (nonexistent) calculations. Following the treatment of DeTar, Brower, and Weis,<sup>16</sup> we assume that the amplitude is (in some sense) dominated by its normal threshold singularities. This assumption has a strong effect on the weights of the various slicings, for double discontinuities across normal thresholds in overlapping-channel invariants vanish.

This assumption is valid in the dual resonance model which has no cuts, only poles, in the channel

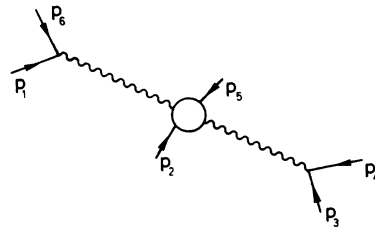


FIG. 11. The six-point function in the helicity limit whose two-Reggeon-two-particle vertex is relevant to the double-Regge cut.

invariants. A single discontinuity leaves a sum of residues, but they are just numbers and lack discontinuities in overlapping channels. Further, a dual model planar as in Fig. 11 has a nonvanishing third double-spectral function: It has singularities in both  $M^2$  and  $u$ , and so the residue of the fixed pole is not zero.

Although the dual model has no cuts, its resonances lie along the real axis of the kinematic variables, in the same place that normal threshold branch points would be found if the amplitude had them. The poles can be thought of as analogs of the normal thresholds. There are no singularities analogous to the higher Landau singularities—triangles or boxes. The dual model is an amplitude dominated by its normal threshold analogs where the domination is absolute: No other singularities exist.

(I should remark that a two-Reggeon cut constructed with dual vertices is not the same thing as a dual loop. It is really a semiphenomenological object, well defined only for  $s \rightarrow \infty$  and all momentum transfers small.)

One can proceed to write down the general form of the six-point function satisfying the above assumptions:

$$A_6 = (-s_{23})^{\alpha(t_2)} (-s_{56})^{\alpha(t_1)} g_1(M^2) + (-s_{12})^{\alpha(t_1)} (-s_{45})^{\alpha(t_2)} g_2(u) + \text{other terms}, \quad (7.3)$$

where  $g(x)$  has right-hand singularities in  $x$  and the "other terms" are entire in  $M^2$  but may have cuts in  $S$ . Performing the  $M^2$  integration in the cut graph by contour wrapping about the  $M^2$  discontinuities, it follows immediately that the slicing through both Reggeons does not contribute to the cut because it lacks  $M^2$  discontinuities: The contour may be closed upon itself to give a weight of zero. [This conclusion assumes that the "other terms" of (7.3) are not constant in  $M^2$ , which would lead to a constant infinity as the weight of the two-Reggeon slice. Such a constant term is a Kronecker  $\delta$  in the  $j$  plane: Such a term is not

analytic in the angular momentum and cannot be reproduced by a Froissart-Gribov projection and Sommerfeld-Watson transform. Following conventional analyses<sup>17</sup> of the cut, we assume such terms are absent.] Further, each of the slicings through one Reggeon (which here is a discontinuity in some  $s_{ij}$ ) possesses  $M^2$  singularities only on the right ( $M^2$ ) or left ( $u$ ). The labels are drawn on the  $s_{ij}$ 's only to indicate which slicings are taken. The numerical value of all the  $s$ 's is fixed by (7.2).

The function  $g(M^2)$  of (7.3) may be written as

$$g_1(M^2) + g_2(u) = \sum_i \frac{1}{-2\pi i} \frac{\Gamma_i}{M^2 - m_i^2 + i\epsilon} + \sum_{i'} \frac{1}{-2\pi i} \frac{\Gamma_{i'}}{u - u_{i'} + i\epsilon}, \quad (7.4)$$

which is only an asymptotic expansion for the general multi-Regge amplitude but is exact (in the Mittag-Leffler sense) for the dual model. The Mandelstam vertex has a similar form for large  $M^2$ : The vertex as a function of  $M^2$  looks like

$$B(M^2) = \int \frac{d\alpha_1 d^2 q_{\perp} f_1(\mu' s)}{M_{\perp}^2 - \mu_1^2/\alpha_1 - \mu_2^2/(1-\alpha_1) + i\epsilon} + \int \frac{d\alpha_1 d^2 q_{\perp} f_2(\mu' s)}{M_{\perp}^2 + \mu_5^2/(1-\alpha_1) + \mu_6^2/\alpha_1 + 2d^2 - i\epsilon} \sim \frac{1}{M^2} \int d\alpha d^2 q_{\perp} f_1(\mu' s) + \frac{1}{u} \int d\alpha d^2 q_{\perp} f_2(\mu' s) \quad (7.5)$$

as  $M^2$  becomes large.

Now the discontinuities of the four-point amplitude may be calculated. The simplest approach is again via Sudakov variables. Write  $M_1^2 = \alpha_1 \beta_1 s$  and  $M_2^2 = \alpha_2 \beta_2 s$ , and then the four-point function becomes

$$A(s, t) = \int \frac{dt_1 dt_2 \theta(-\lambda)}{\sqrt{-\lambda}} (-i \xi_1 \xi_2) s^{\alpha_1 + \alpha_2 - 1} I(s),$$

where

$$I(s) = \frac{s^2}{(-2\pi i)^2} \sum_{i,j} \int d\alpha_1 d\beta_1 d\alpha_2 d\beta_2 \delta(1 - \alpha_1 - \alpha_2) \delta(1 - \beta_1 - \beta_2) \times \left[ \frac{\Gamma_i}{\alpha_1 \beta_1 s - m_i^2 + i\epsilon} + (M_1^2 - u_1) \right] \left[ \frac{\Gamma_j}{\alpha_2 \beta_2 s - m_j^2 + i\epsilon} + (M_2^2 - u_2) \right]. \quad (7.6)$$

After eliminating  $\alpha_2$ ,  $\beta_1$ , and the  $\delta$  functions, the slicings can be computed. Taking a discontinuity of  $A(s, t)$  is equivalent to slicing  $I(s)$  and altering the signature and closed-loop  $i$  structure. This is another example of the techniques of Sec. II.

The two diffractive slicings are calculated by requiring that the two  $M^2$  or two  $u$  singularities pinch the  $\alpha$ ,  $\beta$  hypercontour. Consider the  $M^2$  pinch. Following the rules of Sec. II, we see that it can only happen for  $0 < \alpha_1 < 1$  and  $0 < \beta_2 < 1$ , so



that

$$\begin{aligned}
 [\text{disc}_s I(s)]_{\text{diff}} &= s^2 \sum_{i,j} \Gamma_i \Gamma_j \\
 &\times \int_0^1 d\alpha_1 \\
 &\times \int_0^1 d\beta_2 \delta(\alpha_1(1-\beta_2)s - m_i^2) \\
 &\times \delta((1-\alpha_1)\beta_2s - m_j^2) \quad (7.7)
 \end{aligned}$$

$$\begin{aligned}
 &= s \sum_{i,j} \Gamma_i \Gamma_j \int_0^1 \frac{d\alpha_1}{\alpha_1(1-\alpha_1)} \\
 &\times \delta\left(s - \frac{m_i^2}{\alpha_1} - \frac{m_j^2}{1-\alpha_1}\right) \quad (7.8)
 \end{aligned}$$

$$\begin{aligned}
 &= \sum_{i,j} \Gamma_i \Gamma_j \int dM_1^2 dM_2^2 \delta(M_1^2 - m_i^2) \\
 &\times \delta(M_2^2 - m_j^2) \quad (7.9)
 \end{aligned}$$

---


$$\text{disc}_{s_{23}} I(s) = s^2 \sum_{i,j} \frac{\Gamma_i \Gamma_j}{(-2\pi i)^2} \int_{-\infty}^{\infty} \frac{d\alpha_1 d\beta_2}{[\alpha_1(1-\beta_2)s - m_i^2 + i\epsilon][ (1-\alpha_1)\beta_2s - m_j^2 + i\epsilon]}. \quad (7.12)$$

The integrations must be done in order: If the  $\beta_2$  integration is not to vanish, poles must lie on opposite sides of the  $\beta_2$  real axis, so  $0 < \alpha_1 < 1$ . Encircling one of the poles gives

$$\begin{aligned}
 \text{disc}_{s_{23}} I(s) &= s \sum_{i,j} \frac{\Gamma_i \Gamma_j}{-2\pi i} \int_0^1 \frac{d\alpha_1}{\alpha_1(1-\alpha_1)} \\
 &\times \left( s - \frac{m_i^2}{\alpha_1} - \frac{m_j^2}{1-\alpha_1} + i\epsilon \right)^{-1} \quad (7.13)
 \end{aligned}$$

or

$$\text{disc}_s [\text{disc}_{s_{23}} I(s)] = [\text{disc}_s I(s)]_{\text{diff}}. \quad (7.14)$$

So if

$$\text{disc}_{s_{23}} I(s) = \tilde{I}_1(s) + i\tilde{I}_2(s),$$

then

$$\begin{aligned}
 \tilde{I}_2(s) &= \frac{1}{2i} [\text{disc}_s I(s)]_{\text{diff}} \\
 &= \frac{1}{2i} N_1 N_2. \quad (7.15)
 \end{aligned}$$

If the Reggeons have positive signature (pure imaginary  $\xi$ ), it is not necessary to calculate the real part of  $\text{disc}_{s_{23}} I(s)$  in order to find the weight of the absorption slicings. The reason is that there is another slice through a Reggeon which has only right-hand singularities in  $M_1^2$  and  $M_2^2$  but different signature factors: that is through

$$= \left( \sum_i \Gamma_i \right) \left( \sum_j \Gamma_j \right) = N_1 N_2, \quad (7.10)$$

changing variables back to  $M_1^2$  and  $M_2^2$ , performing the integrations, and summing over the residues. A result for the  $u$  discontinuity is found to be identical to (7.10) (for the same reason that the  $u$  and  $M^2$  discontinuities are equal in the Mandelstam graph). The two diffractive slicings give a weight

$$\begin{aligned}
 (2 \text{Im} A)_{\text{diff}} &= \int \frac{dt_1 dt_2 \theta(-\lambda)}{\sqrt{-\lambda}} N_1 N_2 (-s)^{\alpha_1 + \alpha_2 - 1} \\
 &\times (\xi_1 \xi_2^* + \xi_1^* \xi_2). \quad (7.11)
 \end{aligned}$$

Now we turn to the four absorptive slicings. Because of the form of (7.3) one of the sums of resonances in (7.4) is eliminated by the slice: Assume, for example, that  $s_{23}$  is sliced and the  $u$ -channel resonances disappear. Then

---

$s_{56}$ . If both Reggeons are identical, these two slicings must be considered simultaneously under the class of discontinuities which preserve the  $M^2$  normal thresholds.

The two sliced  $I(s)$ 's and their associated signature factors are

$$\begin{aligned}
 \text{disc}_{s_{23}} I(s) \times (\text{signature}) &= -i(2i \text{Im} \xi_1)(\xi_2)^* \\
 &\times i(\tilde{I}_1 + i\tilde{I}_2), \quad (7.16a)
 \end{aligned}$$

$$\begin{aligned}
 \text{disc}_{s_{56}} I(s) \times (\text{signature}) &= +i(2i \text{Im} \xi_2)(\xi_1) \\
 &\times (-i)(\tilde{I}_1 - i\tilde{I}_2). \quad (7.16b)
 \end{aligned}$$

The first  $i$  is for the closed Reggeon loop and is complex-conjugated in going to (7.16b) because the closed loop lies on the opposite side of the slice. The function  $i(\tilde{I}_1 + i\tilde{I}_2)$  is complex-conjugated in (7.16b) because the two propagators now lie on the opposite side of the slice and their  $i\epsilon$ 's are reversed by complex conjugation. (Reference to Fig. 8 may be helpful in visualizing these changes.) The two expressions sum to

$$\begin{aligned}
 \text{disc}_s I(s) \times (\text{signature}) &= 2i\tilde{I}_1(\text{Im} \xi_1 \text{Re} \xi_2 + \text{Re} \xi_1 \text{Im} \xi_2) \\
 &- 4i\tilde{I}_2[\text{Im} \xi_1 \text{Im} \xi_2 \\
 &- \frac{1}{2}i(\text{Im} \xi_1 \text{Re} \xi_2 - \text{Im} \xi_2 \text{Re} \xi_1)]. \quad (7.17)
 \end{aligned}$$

For positive-signature Reggeons the terms multi-

plying  $\bar{I}_1$  vanish. The surviving term is

$$-4(N_1 N_2 / 2) \text{Im } \xi_1 \text{Im } \xi_2. \quad (7.18)$$

Similar arguments combine the two slicings which preserve the  $u$ -channel discontinuities into another factor identical to (7.18), so that the sum of slices through no Reggeons and one Reggeon add up to give

$$2 \text{Im} A(s, t) = \int \frac{dt_1 dt_2 \theta(-\lambda)}{\sqrt{-\lambda}} N_1 N_2 (s)^{\alpha_1 + \alpha_2 - 1} \\ \times (\xi_1 \xi_2^* + \xi_2 \xi_1^* - 4 \text{Im } \xi_1 \text{Im } \xi_2), \quad (7.19)$$

which again reserves the sign of the cut for positive-signature Reggeons; however, the counting is  $2 - 4 = -2$ .

So we see that different sets of intermediate states build up the two-Reggeon cut in a model with cuts but no poles (the Mandelstam graph) and in a model with poles but no cuts (the dual model). The difference in the two results happens because of the difference in strength of the higher-order Landau singularities in the vertices. In both these models the singularity structure of the vertex is known unambiguously. The situation for an arbitrary multi-Regge vertex is much less clear. The problem is that in these various slicings the results of theorems about double discontinuities can only be applied after the  $M^2$  contour rotation has been performed. They are only valid close to the physical region of the  $M^2$  plane. There is no guarantee that some other kind of singularity will not be encountered at complex  $M^2$  which must be considered in addition to the integral of the  $M^2$  normal-threshold discontinuity. Indeed, these relations hold for the Mandelstam graph—for instance, the slice through both Reggeons eliminates the  $M^2$  normal threshold—but other singularities appear in the complex plane to compensate. The part of the counting in that case due to normal thresholds is identical to the result we have found here,  $2 - 4 = -2$ .

What does this result imply for the Reggeon calculus? It would seem that there is no unique Reggeon calculus, that one can build Reggeon calculuses which have similar  $j$ -plane properties but have rather different energy-plane behavior. In fact, the energy-plane behavior desired by physical reasoning selects a particular form of the vertices and gives a Reggeon calculus for one kind of scattering different properties from one which describes the scattering of a different class of particles.

Consider first the high-energy scattering of nuclei. It is plausible, for instance, that in deu-

teron-deuteron scattering the deuterons could disassociate into protons and neutrons which could then scatter independently off one another. Further, it is not a bad approximation to regard the nucleons in a nucleus as weakly interacting (phenomenologically) fundamental fields. A Reggeon calculus with field-theoretic particle-Reggeon vertices would probably provide a good description of these processes. It would obey the counting rules of Abramovskii *et al.* for the particle-Reggeon vertices. However, there is still no reason to expect that the Reggeon-Reggeon vertices would have a field-theoretic structure, and so the counting rules for these vertices might differ from those of the particle-Reggeon ones. At any rate, here is a case where, because the binding energy of the nuclei is so small, the triangle and higher-order Landau vertices lie very close to the physical sheet and must be taken into consideration in calculations.

A second example is not strictly a Reggeon calculus but involves Regge cut amplitudes: corrections to wide-angle hadronic scattering. Here one imagines that the hadrons are made out of weakly interacting fundamental fields, the partons, and the Mandelstam graph is a model for, say,  $\pi$ - $\pi$  scattering. One can imagine scattering of several constituents of the hadrons at once, leading to polyperipheral final states: the field-theoretic vertices again lead to a counting of  $2 - 8 + 4$ . Again, in higher-order processes slicing several-Reggeon couplings might give different results than in Ref. 5.

The situation is quite different for hadronic scattering in the forward direction. The richness of the hadronic mass spectrum suggests that the Reggeon-particle vertex is dominated (in some sense) by its resonance poles and normal threshold branch cuts. While it is possible that the proton could disassociate virtually into a proton and a pion so that a polyperipheral reaction could occur in a  $pp$  collision in the manner of Mandelstam, the proton must move 200 MeV off the mass shell for this to happen; One would not expect this channel to be nearly as important as the corresponding deuteron disassociation. Indeed, because of the large pion-nucleon coupling constant, one would not regard the pion and nucleon as free and noninteracting. One might want to say instead that the proton had become a virtual  $N^*$ . So in the scattering of systems of baryon number 1 or 0, a better description of nature might be via vertices abstracted from the dual model. A 2-to- $n$  amplitude would be (in two-component language) a sum of multiperipheral and diffractive production which included elastic rescattering corrections. The square of the production amplitude

would give a Reggeon calculus with a  $j$ -plane structure similar to that of a field-theoretic vertex calculus, although the  $s$ -channel behavior would be quite different.

It seems that writing down a Reggeon calculus for two-to-two scattering does not lead to the domination of two-to- $n$  production amplitudes by a unique set of processes. Rather, the reverse is true. The most general statement that one can make about the sum of slices of the two-Reggeon cut is that the sign reversal takes the form

$$-R = R - 2(R + x) + 2x,$$

with  $x$  strongly dependent on the presence and importance of the higher-order Landau singularities in the vertices, and hence on the nature of target and projectile:  $x \approx R$  in the scattering of nuclei,  $x \approx 0$  in the scattering of objects of baryon number 1 or 0.

The calculation of the imaginary part of the two-

Reggeon cut amplitude by unitarity and the determination of which production processes are important in generating the cut is extremely ambiguous. Not only is the internal structure of the Reggeon important; the result depends critically on the analytic properties of the Reggeon-particle vertices throughout the complex plane.

#### ACKNOWLEDGMENT

I would like to thank my advisor, Professor Carleton DeTar, for suggesting this problem, and for much valuable advice about it. Conversations and correspondence with Dr. I. Halliday, Dr. P. Landshoff, Dr. C. Sachrajda, and Dr. G. Winbow were useful in its conclusion. Finally, I am grateful to the Department of Theoretical Physics of the University of Geneva for its hospitality during the completion of this work.

\*This work is supported in part through funds provided by the Atomic Energy Commission under Contract No. AT(11-1)-3069.

†National Science Foundation Graduate Fellow.

‡Present address.

<sup>1</sup>D. Amati, S. Fubini, and A. Stanghellini, *Nuovo Cimento* **26**, 896 (1962).

<sup>2</sup>S. Mandelstam, *Nuovo Cimento* **30**, 1127 (1963); **30**, 1148 (1963).

<sup>3</sup>V. N. Gribov, I. Ya. Pomeranchuk, and K. A. Ter-Martirosyan, *Yad. Fiz.* **2**, 361 (1965) [*Sov. J. Nucl. Phys.* **2**, 258 (1965)]; *Phys. Rev.* **139**, B184 (1965).

<sup>4</sup>A. R. White, *Nucl. Phys.* **B50**, 93 (1972); **B50**, 130 (1972).

<sup>5</sup>V. A. Abramovskii, O. V. Kancheli, and V. N. Gribov, in *Proceedings of the XVI International Conference on High Energy Physics, Chicago-Batavia, Ill., 1972*, edited by J. D. Jackson and A. Roberts (NAL, Batavia, Ill., 1973), Vol. I, p. 389.

<sup>6</sup>T. G. Halliday and C. T. Sachrajda, *Phys. Rev. D* **8**, 3598 (1973).

<sup>7</sup>Cf. O. Steinmann, *Helv. Phys. Acta* **33**, 275 (1960); **33**, 347 (1960); H. P. Stapp, *Phys. Rev. D* **3**, 3177 (1971).

<sup>8</sup>V. Sudakov, *Zh. Eksp. Teor. Fiz.* **30**, 87 (1956) [*Sov. Phys.—JETP* **3**, 65 (1956)].

<sup>9</sup>H. Rothe, *Phys. Rev.* **159**, 1471 (1967).

<sup>10</sup>R. J. Eden, P. V. Landshoff, D. I. Olive, and J. Polkinghorne, *The Analytic S-Matrix* (Cambridge Univ. Press, Cambridge, England, 1966).

<sup>11</sup>G. M. Cicuta and R. L. Sugar, *Phys. Rev. D* **3**, 910 (1971).

<sup>12</sup>B. Hasslacher and D. K. Sinclair, *Phys. Rev. D* **3**, 1770 (1971).

<sup>13</sup>V. N. Gribov, *Zh. Eksp. Teor. Fiz.* **53**, 654 (1968) [*Sov. Phys.—JETP* **26**, 414 (1968)].

<sup>14</sup>I. J. Muzinich, F. E. Paige, T. L. Trueman, and L.-L. Wang, *Phys. Rev. Lett.* **28**, 850 (1972).

<sup>15</sup>A. Capella and J. Kaplan, *Nucl. Phys.* **B79**, 141 (1974).

<sup>16</sup>R. C. Brower, C. E. DeTar, and J. H. Weis, *Phys. Rep.* **14C**, 257 (1974).

<sup>17</sup>C. E. DeTar, *Phys. Rev. D* **11**, 866 (1975).